Imaging Science in Dentistry 2021; 51: 73-80
https://doi.org/10.5624/isd.20200230

CBCT imaging and histopathological characteristics of osteoradionecrosis and medication-related osteonecrosis of the jaw

Ichiro Ogura[1,*], Yoshiyuki Minami[1], Junya Ono[2], Yoriaki Kanri[2], Yasuo Okada[2], Kensuke Igarashi[3], Maiko Haga-Tsujimura[4,5], Ken Nakahara[5], Eizaburo Kobayashi[6]

[1]*Department of Oral and Maxillofacial Radiology, The Nippon Dental University School of Life Dentistry at Niigata, Niigata, Japan*
[2]*Department of Pathology, The Nippon Dental University School of Life Dentistry at Niigata, Niigata, Japan*
[3]*Department of Dental Materials Science, The Nippon Dental University School of Life Dentistry at Niigata, Niigata, Japan*
[4]*Department of Histology, The Nippon Dental University School of Life Dentistry at Niigata, Niigata, Japan*
[5]*Advanced Research Center, The Nippon Dental University School of Life Dentistry at Niigata, Niigata, Japan*
[6]*Department of Oral and Maxillofacial Surgery, The Nippon Dental University School of Life Dentistry at Niigata, Niigata, Japan*

ABSTRACT

Purpose: The purpose of this study was to evaluate the cone-beam computed tomographic (CBCT) imaging and histopathological characteristics of osteoradionecrosis (ORN) and medication-related osteonecrosis of the jaw (MRONJ).
Materials and Methods: Ten surgical specimens from segmental mandibulectomy (3 ORN and 7 MRONJ) were analyzed using CBCT. The CBCT parameters were as follows: high-resolution mode (tube voltage, 90.0 kV; tube current, 4.00 mA; rotation time, 16.8 s; field of view, 56 mm × 56 mm; thickness, 0.099 mm). Histopathological characteristics were evaluated using histological slides of the surgical specimens. The Pearson chi-square test was used to compare ORN and MRONJ in terms of CBCT findings (internal texture, sequestrum, periosteal reaction and cortical perforation) and histopathological characteristics (necrotic bone, inflammatory cells, reactive bone formation, bacteria, *Actinomyces*, and osteoclasts). A P value less than 0.05 was considered to indicate statistical significance.
Results: MRONJ showed periosteal reaction on CBCT more frequently than ORN (7 of 7 [100%] vs. 0 of 3 [0%], $P<0.05$). Regarding histopathological characteristics, MRONJ showed osteoclasts more frequently than ORN (6 of 7 [85.7%] vs. 0 of 3 [0%], $P<0.05$).
Conclusion: This study evaluated the CBCT imaging and histopathological characteristics of ORN and MRONJ, and the findings suggest that CBCT could be useful for the evaluation of ORN and MRONJ. ***(Imaging Sci Dent 2021; 51: 73-80)***

KEY WORDS: Bisphosphonate-Associated Osteonecrosis of the Jaw; Osteoradionecrosis; Cone-Beam Computed Tomography

Introduction

Medication-related osteonecrosis of the jaw (MRONJ) is a well-known complication of treatment with bisphosphonates, denosumab, and other drugs, such as anti-angiogenic agents and novel anti-cancer drugs. The diagnosis of MRONJ is currently based on clinical parameters alone.[1]

This work was supported by JSPS KAKENHI Grant Number JP 18K09754.
Received August 31, 2020; Revised October 14, 2020; Accepted October 28, 2020
*Correspondence to : Prof. Ichiro Ogura
Department of Oral and Maxillofacial Radiology, The Nippon Dental University School of Life Dentistry at Niigata, 1-8 Hamaura-cho, Chuo-ku, Niigata, Niigata 951-8580, Japan
Tel) 81-25-267-1500, E-mail) ogura@ngt.ndu.ac.jp

Osteoradionecrosis (ORN) is a pernicious complication of radiotherapy in head and neck cancer. The mechanism of pathogenesis is still under investigation, although the most frequently reported cause is radiation arteritis.[2] Histological analysis and radiographic features are not considered mandatory for these diagnoses, and most patients do not undergo a biopsy from the exposed necrotic bone.[3]

Multimodal imaging, such as panoramic radiography,[4] scintigraphy, multidetector computed tomography (MDCT), magnetic resonance imaging,[5-8] and single-photon emission computed tomography-computed tomography[9,10] are useful for detecting MRONJ and ORN. Furthermore, cone-

beam computed tomography (CBCT) provides accurate anatomical details in 3-dimensional and multiplanar reformation images for diagnosis and treatment planning.[11-15] Evaluating surgical specimens of MRONJ and ORN with CBCT is important because it assists in preparing pathological specimens and reassessing the surgical margin. Furthermore, compared with MDCT, CBCT is easy to perform, with short acquisition scan times and high resolution.[16] However, to the best of the authors' knowledge, little has been published in the literature on the usefulness of CBCT for the evaluation of surgical specimens of ORN and MRONJ.[17,18] The purpose of this study was to evaluate the CBCT imaging and histopathological characteristics of ORN and MRONJ.

Materials and Methods

Subjects

This study was approved by the ethics committee of our university (approval no. ECNG-R-318). After patients provided written informed consent, 10 surgical specimens of segmental mandibulectomy (3 ORN; 3 men; mean age, 71.0 years; range, 54-85 years and 7 MRONJ [all stage 3]: 2 men and 5 women; mean age, 77.1 years; range 56-86 years) were analyzed using CBCT at the authors' university hospital from September 2017 to January 2020. Patients were diagnosed with MRONJ based on the criteria presented in the 2014 American Association of Oral and Maxillofacial Surgeons position paper.[1]

CBCT studies

CBCT imaging of surgical specimens was performed with a CBCT unit (Fine Cube; Yoshida, Tokyo, Japan). Surgical specimens in 10% formaldehyde neutral buffer solution were fixed on the chinrest for CBCT (Fig. 1) and examined following the hospital's protocol.[18] The CBCT parameters were as follows: high-resolution mode (tube voltage, 90.0 kV; tube current, 4.00 mA; rotation time, 16.8 s; field of view, 56 mm × 56 mm; thickness, 0.099 mm).

One oral and maxillofacial radiologist, with over 20 years of experience, reviewed all images. The following CBCT findings were evaluated: internal texture (normal, sclerotic, lytic, and sclerotic), the presence of a sequestrum, periosteal reaction, and cortical perforation (buccal, lingual, and inferior).

Histopathological studies

Three oral and maxillofacial pathologists reviewed all histological slides. All archival slides were stained with hematoxylin and eosin. In all cases in which bacteria were evident on hematoxylin and eosin staining, periodic acid-Schiff (PAS), Gram, and Grocott stains were added.

The set of parameters evaluated in the histomorphometric analysis included the presence or absence of necrotic bone, inflammation, reactive bone formation, bacteria (based on PAS, Gram, and Grocott stains) and osteoclasts. To measure inflammation, the percentage of the bone circumference surrounded by inflammatory cells was evaluated in a semi-quantitative manner on the 5-tier scale from 0 to 4 proposed by Shuster et al.,[3] as follows: 0 = absence of inflammatory cells; 1 = inflammatory cells surrounding up to 10% of the bone circumference; 2 = inflammatory cells surrounding 10%-25% of the bone circumference; 3 = inflammatory cells surrounding 25%-50% of the bone circumference; 4 = inflammatory cells surrounding > 50% of the bone circumference. The inflammatory infiltrate was examined

Fig. 1. Cone-beam computed tomography (CBCT) unit. A surgical specimen of the jaw is fixed to the chin rest for CBCT.

Table 1. Data on patients with osteonecrosis and CBCT findings of the surgical specimens

Case	Age (years)	Sex	Osteonecrosis	Underlying disease	Medication or radiotherapy	CBCT finding			
						Internal texture	Sequestrum	Periosteal reaction	Cortical perforation
1	86	Female	MRONJ	Osteoporosis	Alendronate	Lytic and sclerotic	Present	Lingual and inferior	Lingual and inferior
2	85	Female	MRONJ	Osteoporosis	Alendronate	Lytic and sclerotic	Present	Buccal and lingual	Buccal and lingual
3	85	Female	MRONJ	Osteoporosis	Minodronate	Lytic and sclerotic	Present	Buccal and lingual	Buccal and lingual
4	82	Female	MRONJ	Osteoporosis	Minodronate	Sclerotic	Absent	Buccal	Buccal
5	65	Male	MRONJ	Osteoporosis	Minodronate	Lytic and sclerotic	Present	Buccal	Buccal
6	81	Male	MRONJ	Rheumatism	Minodronate	Lytic and sclerotic	Present	Buccal and lingual	Buccal and lingual
7	56	Female	MRONJ	Breast cancer	Denosumab to Zoledronate	Lytic and sclerotic	Absent	Buccal, lingual, and inferior	Buccal, lingual, and inferior
8	85	Male	ORN	Oropharyngeal cancer	Radiotherapy	Lytic and sclerotic	Present	None	Buccal and lingual
9	74	Male	ORN	Maxillary cancer	Radiotherapy	Lytic and sclerotic	Present	None	Buccal, lingual, and inferior
10	54	Male	ORN	Tongue cancer	Radiotherapy	Lytic and sclerotic	Absent	None	Buccal, lingual, and inferior

CBCT: cone-beam computed tomography, MRONJ: medication-related osteonecrosis of the jaw, ORN: osteoradionecrosis

under ×10 magnification. Each slide was searched for the area with the highest density of inflammation and the score was assigned accordingly.

Statistical analysis

The Pearson chi-square test was used to compare ORN and MRONJ in terms of the CBCT findings and histopathological characteristics. The statistical analysis was performed with SPSS version 26 (IBM Japan, Tokyo, Japan). A P value less than 0.05 was considered to indicate statistical significance.

Results

Table 1 presents data on the patients with osteonecrosis and the CBCT findings of the surgical specimens. For MRONJ (case 3, Fig. 2), the CBCT findings included lytic and sclerotic internal texture, presence of a sequestrum, and buccal and lingual periosteal reaction and cortical perforation. The CBCT findings of ORN (case 9, Fig. 3) included lytic and sclerotic internal texture, presence of a sequestrum, no periosteal reaction, and buccal, lingual, and inferior cortical perforation.

The presence of a sequestrum was observed more frequently in MRONJ than in ORN (5 of 7 [71.4%] vs. 2 of 3 [66.7%], $P>0.05$). MRONJ showed periosteal reaction more frequently than ORN (7 of 7 [100%] vs. 0 of 3 [0%], $P<0.05$). Buccal, lingual, and inferior cortical perforation was found more frequently in ORN than in MRONJ (2 of 3 [66.7%] vs. 1 of 7 [14.3%], $P>0.05$).

Table 2 shows the histopathological characteristics of osteonecrosis in the surgical specimens. The histopathological characteristics of MRONJ (case 3, Figs. 4 and 5) included necrotic bone and granulation tissue with the bone circumference surrounded by inflammatory cells. Six cases of MRONJ (6 of 7, 85.7%) revealed bacteria (mostly Gram-positive, but some Gram-negative). In MRONJ, osteoclasts were rarely found around necrotic bone; however, osteoclasts were found on the bone surface in contact with granulation tissue. Reactive bone formation was observed on destroyed and perforated bone, and on the outside of the cortical bone. In ORN (case 9, Figs. 6 and 7), the histopathological findings showed necrotic bone and granulation tissue with the bone circumference surrounded by abscess

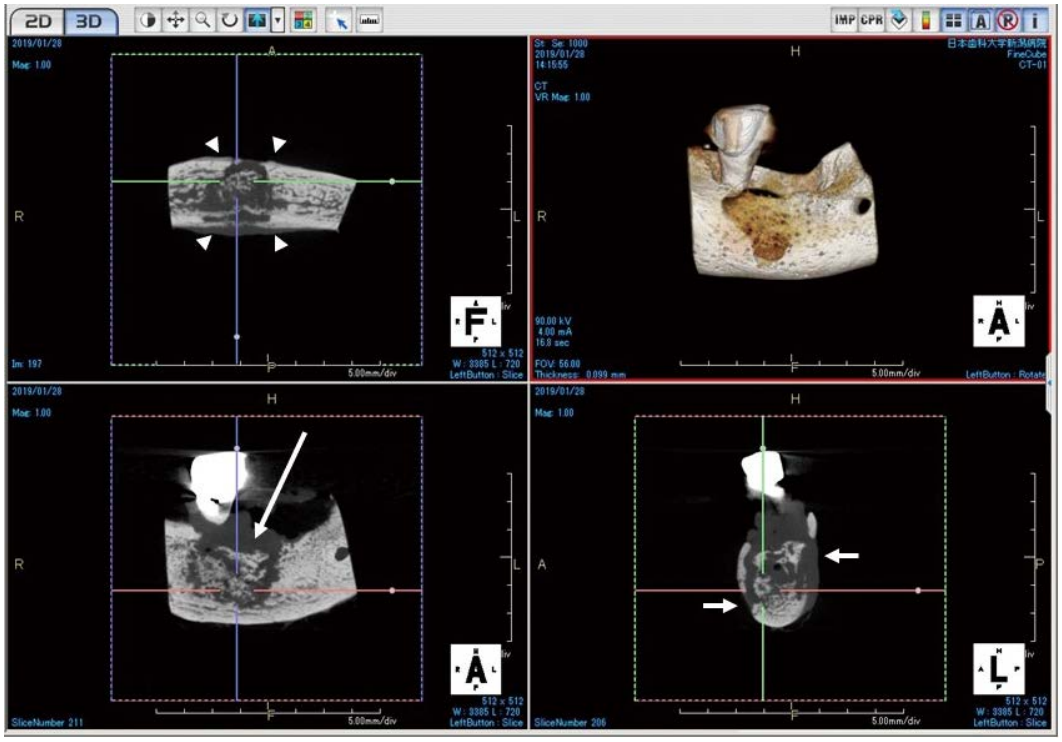

Fig. 2. Cone-beam computed tomographic (CBCT) images of surgical specimen medication-related osteonecrosis of the jaw (case 3). The CBCT findings show lytic and sclerotic internal texture, the presence of a sequestrum (long arrow), and buccal and lingual periosteal reaction (arrowheads) and cortical perforation (short arrows).

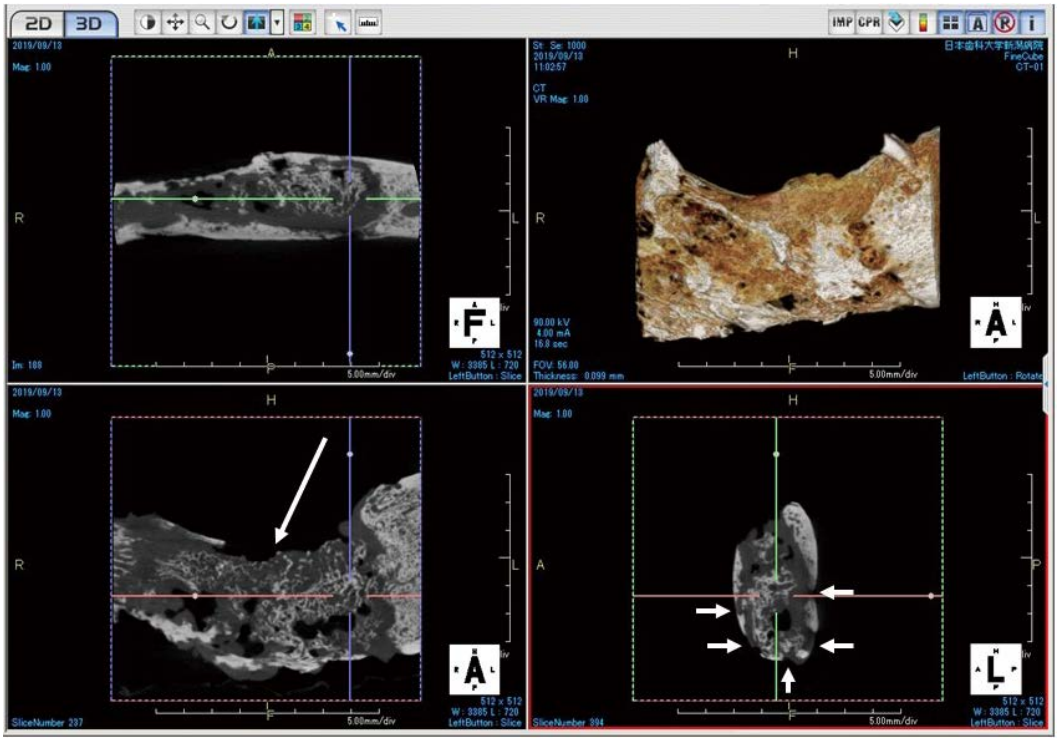

Fig. 3. Cone-beam computed tomographic (CBCT) images of a surgical specimen of osteoradionecrosis of the jaw (case 9). The CBCT findings show lytic and sclerotic internal texture, the presence of a sequestrum (long arrow), no periosteal reaction, and buccal, lingual, and inferior cortical perforation (short arrows).

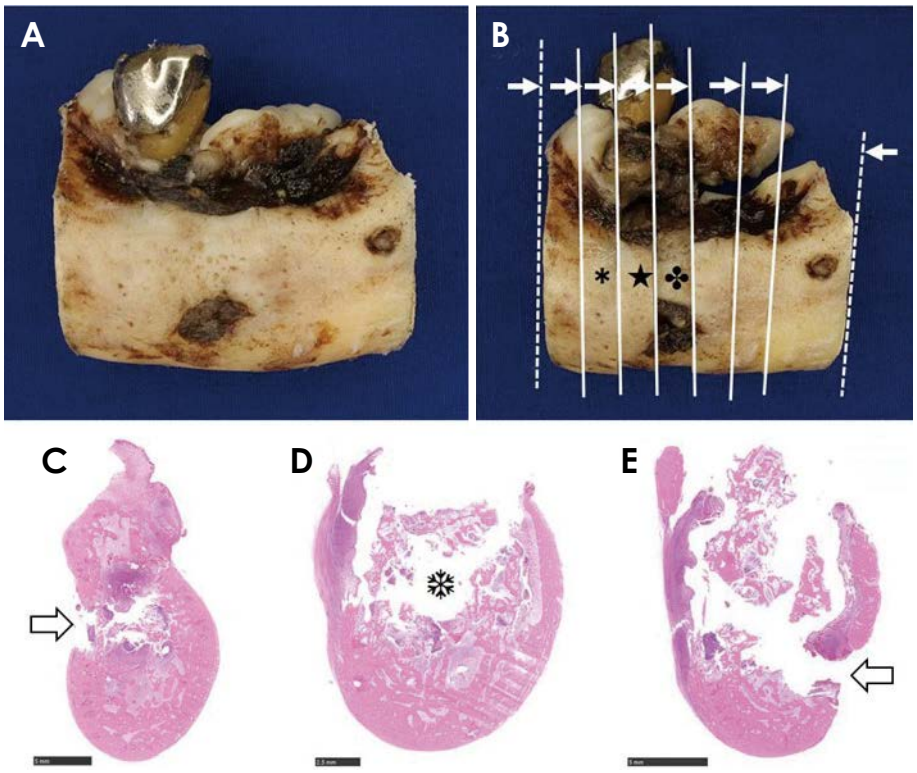

Fig. 4. Histopathological characteristics of a surgical specimen of medication-related osteonecrosis of the jaw (case 3). A. Surgical specimen (buccal side) shows cortical perforation. B. Preparation of the pathological specimen based on the cone-beam computed tomographic (CBCT) findings (arrows, view side). C. Histopathological finding (B*, H&E stain, bar = 5 mm). Lingual side (arrow) shows cortical perforation. D. Histopathological findings (B★, H&E stain, bar = 2.5 mm). The space (❄) is the tooth root. E. Histopathological findings (B✤, H&E stain, bar = 5 mm) corresponding to the coronal CBCT image in Figure 2. The buccal side (arrow) shows cortical perforation.

Table 2. Histopathological characteristics of osteonecrosis in the surgical specimens

Case	Necrotic bone	Inflammatory cells	Reactive bone formation	Bacteria	*Actinomyces*	Osteoclasts
1	Present	25%-50%	Present	G+, G−	Absent	Present
2	Present	Up to 10% of bone circumference	Present	G+, G−	Present	Present
3	Present	25%-50%	Present	G+, G−	Present	Present
4	Present	Up to 10% of bone circumference	Present	None	Absent	Absent
5	Present	25%-50%	Present	G+, G−	Present	Present
6	Present	>50%	Present	G+, G−	Present	Present
7	Present	>50%	Present	G+, G−	Absent	Present
8	Present	Up to 10% of bone circumference	Present	G+, G−	Present	Absent
9	Present	10%-25%	Present	G+, G−	Present	Absent
10	Present	Up to 10% of bone circumference	Absent	G+, G−	Absent	Absent

G+: Gram-positive, G−: Gram-negative

and inflammatory cells. All cases of ORN (3 of 3, 100%) revealed bacteria (mostly Gram-positive, with some Gram-negative) and fibrosis of granulation tissue. In ORN, osteoclasts were rarely found around necrotic bone.

MRONJ showed reactive bone formation more frequently than ORN (7 of 7 [100%] vs. 2 of 3 [66.7%], $P > 0.05$), whereas ORN showed *Actinomyces* more frequently than MRONJ (2 of 3 [66.7%] vs. 4 of 7 [57.1%], $P > 0.05$). Osteoclasts were observed more frequently in MRONJ than in ORN (6 of 7 [85.7%] vs. 0 of 3 [0%], $P < 0.05$).

Discussion

Radiological examinations, especially using computed tomography, make it possible to estimate the extent of MRONJ more accurately.[16] Ogura et al.[5] reported the characteristics of multimodal imaging of MRONJ, and found that periosteal bone proliferation on MDCT (0.5-mm-thick sections, 1-mm reconstruction) was present in 56.3% of cases (9 of 16). Baba et al.[19] evaluated the CT imaging features of bisphosphonate-related osteonecrosis of the jaw (BRONJ)

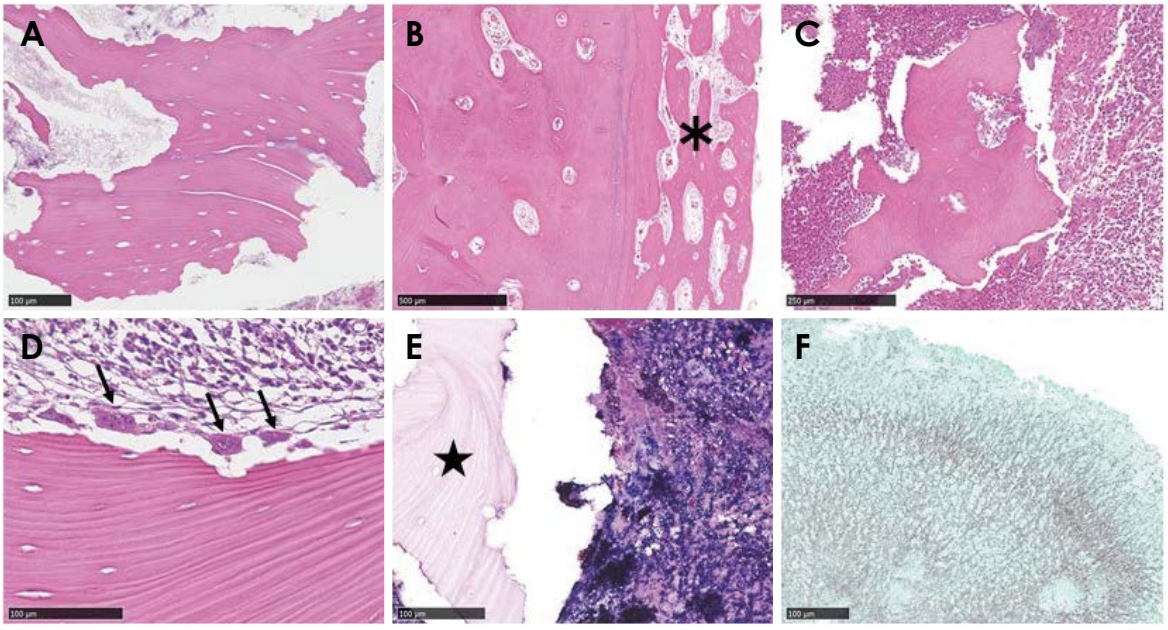

Fig. 5. Histopathological characteristics of a surgical specimen of medication-related osteonecrosis of the jaw (case 3). A. Necrotic bone shows no osteoclasts in resorption lacunae (H&E stain, bar = 100 μm). B. Lateral cortical bone (*) shows reactive bone formation (H&E stain, bar = 500 μm). C. Around the area of necrotic bone, granulation tissue with inflammatory cells is shown (H&E stain, bar = 250 μm). D. Osteoclasts (arrows) are found on the bone surface in contact with the granulation tissue (H&E stain, bar = 100 μm). E. Around the area of necrotic bone (★), bacteria are found (mostly Gram-positive, with some Gram-negative) (Gram stain, bar = 100 μm). F. Bacterial mass shows *Actinomyces* with methenamine silver staining (Grocott stain, bar = 50 μm).

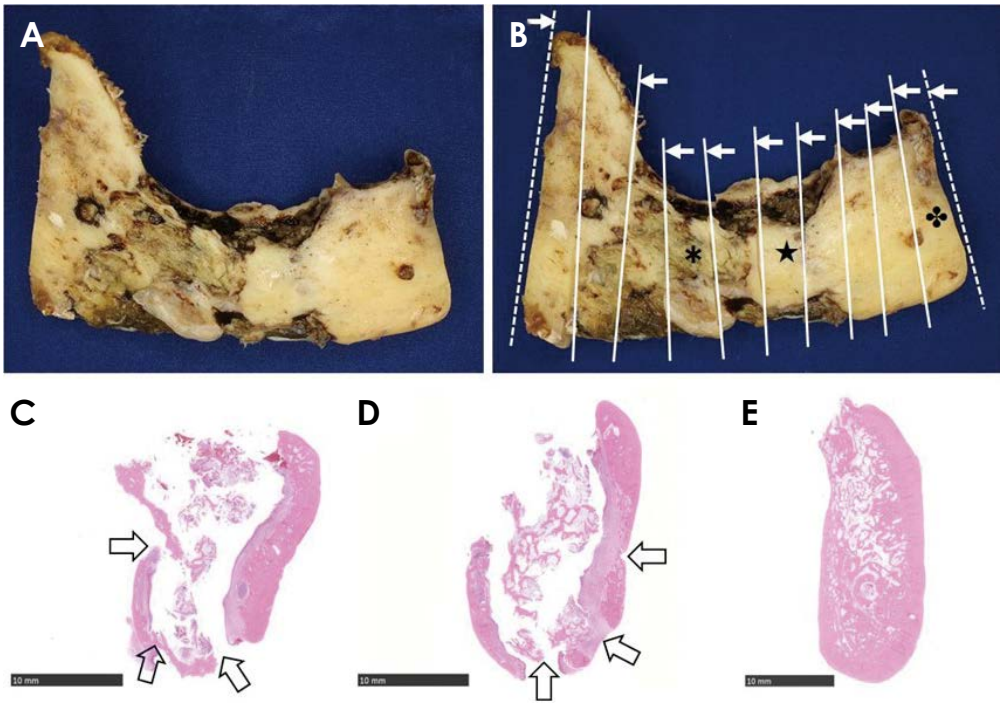

Fig. 6. Histopathological characteristics of a surgical specimen of osteoradionecrosis of the jaw (case 9). A. Surgical specimen (buccal side) shows multiple areas of destroyed and perforated cortical bone. B. Preparation of the pathological specimen based on cone-beam computed tomographic findings (arrows, viewing side). C. Histopathological finding (B*, H&E stain, bar = 10 mm). The buccal and inferior side (arrows) shows cortical destroyed and perforated bone. D. Histopathological finding (B★, H&E stain, bar = 10 mm) corresponding to the coronal CBCT image in Figure 3. Lingual and inferior sides (arrows) show destroyed and perforated cortical bone. E. Histopathological finding of the surgical margin (B✤, H&E stain, bar = 10 mm) shows no necrotic bone or granulation tissue.

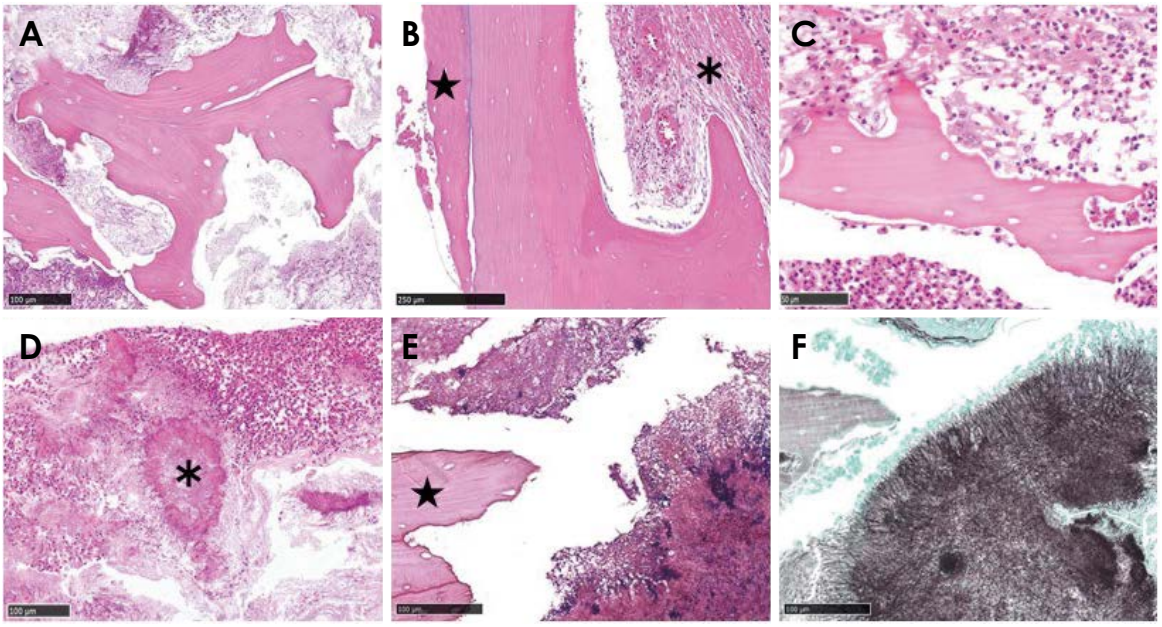

Fig. 7. Histopathological characteristics of a surgical specimen of osteoradionecrosis of the jaw (case 9). A. Necrotic bone shows no osteoclasts in resorption lacunae (H&E stain, bar = 100 μm). B. Reactive bone formation is shown on the lateral cortical bone (★) and fibrosis in the bone marrow (*) (H&E stain, bar = 250 μm). C. Around the area of necrotic bone, abscess and granulation tissue is shown without osteoclasts (H&E stain, bar = 50 μm). D. Inflammatory cells and a bacterial mass (*) are found in the abscess (H&E stain, bar = 100 μm). E. Around the area of necrotic bone (★), bacteria are shown (mostly Gram-positive, with some Gram-negative) (Gram stain, bar = 100 μm). F. The bacterial mass shows *Actinomyces* with methenamine silver staining (Grocott stain, bar = 100 μm).

and denosumab-related osteonecrosis of the jaw (DRONJ), and reported that DRONJ (4 of 10, 40%) showed periosteal reaction more frequently than BRONJ (7 of 65, 10.1%) on MDCT (0.5-mm-thick sections, 2-mm reconstruction). In this study, all cases of BRONJ (6 of 6, 100%) and DRONJ (1 of 1, 100%) showed periosteal reaction on CBCT (0.099 mm thickness). Furthermore, this study found that MRONJ showed periosteal reaction more frequently than ORN on CBCT (7 of 7 (100%) vs. 0 of 3 (0%), $P < 0.05$). We consider that these results can be explained by the higher resolution of CBCT than MDCT, and therefore suggest that evaluations using CBCT are important to assess periosteal reaction as a parameter that may help distinguish between MRONJ and ORN.

Regarding the histopathological characteristics of MRONJ and ORN, Marx et al.[20] reported that BRONJ involves non-inflammatory drug toxicity to bone, with osteoclastic death leading to over-suppression of bone renewal, whereas ORN is another non-inflammatory condition caused by a high linear energy transfer that impairs or kills numerous cell types in the field of radiation, including the periosteum, bone, and all soft tissue. Shuster et al.[3] compared the histopathological characteristics of MRONJ and ORN. They reported that necrotic bone, inflammation, and reactive bone formation were present in both diagnoses, and that osteoclasts were scarce in MRONJ and non-existent in ORN. In the histopathological examinations in this study, MRONJ showed osteoclasts more frequently than ORN (6 of 7 [85.7%] vs. 0 of 3 [0%], $P < 0.05$). Furthermore, six cases of MRONJ (6 of 7, 85.7%) showed bacteria, which were mostly Gram-positive (although some were Gram-negative), while bacteria were not observed in 1 case of MRONJ (case 4). A possible explanation for this finding is that most of the lesion was covered with mucous membranes in the surgical operation, eliminating the exposure of necrotic bone. Osteoclasts were found on the bone surface in contact with granulation tissue, which may have been caused by a vital reaction.

Van Dessel et al.[17] compared the CBCT and micro-CT characteristics of trabecular bone structures in the human mandible, and demonstrated the potential of high-resolution CBCT imaging for *in vivo* applications to quantitative bone morphometry and bone quality assessment. Ogura et al.[18] showed that CBCT, especially the high-resolution mode, is useful for the evaluation of surgical specimens of the jaw. Furthermore, compared with MDCT, CBCT is relatively easy to use, with short acquisition scan times and high resolution. The authors therefore suggest that CBCT could be useful for evaluating surgical specimens in patients with MRONJ and ORN.

There are several limitations of this study. The number of

surgical specimens was small, because few patients underwent segmental mandibulectomy for MRONJ and ORN. However, Zirk et al.[21] showed that CBCT image analyses and volumetric measurements of osteolytic lesions in MRONJ patients were helpful tools for further understanding the clinical appearance of this condition and identifying compromised anatomical landmarks. The authors suggest that evaluating surgical specimens of MRONJ and ORN with CBCT is important because it is helpful for preparing the pathological specimen, reassessing the surgical margin, and predicting the prognosis.

In conclusion, this study evaluated the CBCT imaging and histopathological characteristics of ORN and MRONJ, and found that CBCT could be useful for the evaluation of ORN and MRONJ.

Conflicts of Interest: None

References

1. Ruggiero SL, Dodson TB, Fantasia J, Goodday R, Aghaloo T, Mehrotra B, et al. American Association of Oral and Maxillofacial Surgeons position paper on medication-related osteonecrosis of the jaw - 2014 update. J Oral Maxillofac Surg 2014; 72: 1938-56.
2. Chronopoulos A, Zarra T, Ehrenfeld M, Otto S. Osteoradionecrosis of the jaws: definition, epidemiology, staging and clinical and radiological findings. A concise review. Int Dent J 2018; 68: 22-30.
3. Shuster A, Reiser V, Trejo L, Ianculovici C, Kleinman S, Kaplan I. Comparison of the histopathological characteristics of osteomyelitis, medication-related osteonecrosis of the jaw, and osteoradionecrosis. Int J Oral Maxillofac Surg 2019; 48: 17-22.
4. Ogura I, Kobayashi E, Nakahara K, Haga-Tsujimura M, Igarashi K, Katsumata A. Computer programme to assess mandibular cortex morphology in cases of medication-related osteonecrosis of the jaw with osteoporosis or bone metastases. Imaging Sci Dent 2019; 49: 281-6.
5. Ogura I, Sasaki Y, Kameta A, Sue M, Oda T. Characteristic multimodal imaging of medication-related osteonecrosis of the jaw: comparison between oral and parenteral routes of medication administration. Pol J Radiol 2017; 82: 551-60.
6. Ogura I, Sue M, Oda T, Sasaki Y, Hayama K. Comparison between mandibular malignant tumors and inflammatory lesions using ^{67}Ga scintigraphy: relationship with panoramic radiography, CT and MRI findings. Int J Diagn Imaging 2017; 4: 67-73.
7. Ogura I, Oda T, Sue M, Sasaki Y, Hayama K. Comparison between squamous cell carcinoma and inflammatory diseases of the oral and maxillofacial region using gallium-67 scintigraphy with computed tomography and magnetic resonance imaging. Pol J Radiol 2018; 83: e452-8.
8. Ogura I, Sasaki Y, Sue M, Oda T, Kameta A, Hayama K. Tc-99m hydroxymethylene diphosphonate scintigraphy, computed tomography and magnetic resonance imaging of osteonecrosis in the mandible: osteoradionecrosis versus medication-related osteonecrosis of the jaw. Imaging Sci Dent 2019; 49: 53-8.
9. Ogura I, Kobayashi E, Nakahara K, Igarashi K, Haga-Tsujimura M, Toshima H. Quantitative SPECT/CT imaging for medication-related osteonecrosis of the jaw: a preliminary study using volume-based parameters, comparison with chronic osteomyelitis. Ann Nucl Med 2019; 33: 776-82.
10. Ogura I, Sasaki Y, Sue M, Oda T, Kameta A, Hayama K. Tc-99m hydroxymethylene diphosphonate SPECT/CT for the evaluation of osteonecrosis of the jaw: preliminary study on diagnostic ability of maximum standardized uptake value. Clin Radiol 2020; 75: 46-50.
11. Treister NS, Friedland B, Woo SB. Use of cone-beam computerized tomography for evaluation of bisphosphonate-associated osteonecrosis of the jaws. Oral Surg Oral Med Oral Pathol Oral Radiol Endod 2010; 109: 753-64.
12. Wilde F, Heufelder M, Lorenz K, Liese S, Liese J, Helmrich J, et al. Prevalence of cone beam computed tomography imaging findings according to the clinical stage of bisphosphonate-related osteonecrosis of the jaw. Oral Surg Oral Med Oral Pathol Oral Radiol 2012; 114: 804-11.
13. Kämmerer PW, Thiem D, Eisenbeiß C, Dau M, Schulze RK, Al-Nawas B, et al. Surgical evaluation of panoramic radiography and cone beam computed tomography for therapy planning of bisphosphonate-related osteonecrosis of the jaws. Oral Surg Oral Med Oral Pathol Oral Radiol 2016; 121: 419-24.
14. Sue M, Oda T, Sasaki Y, Ogura I. Age-related changes in the pulp chamber of maxillary and mandibular molars on cone-beam computed tomography images. Oral Radiol 2018; 34: 219-23.
15. Mizuhashi F, Ogura I, Sugawara Y, Oohashi M, Sekiguchi H, Saegusa H. Characteristics of root fractures: image on intraoral radiography, panoramic radiography, and cone-beam computed tomography. Oral Sci Int 2020; 17: 34-8.
16. Leite AF, Ogata Fdos S, de Melo NS, Figueiredo PT. Imaging findings of bisphosphonate-related osteonecrosis of the jaws: a critical review of the quantitative studies. Int J Dent 2014; 2014: 784348.
17. Van Dessel V, Huang Y, Depypere M, Rubira-Bullen I, Maes F, Jacobs R. A comparative evaluation of cone beam CT and micro-CT on trabecular bone structures in the human mandible. Dentomaxillofac Radiol 2013; 42: 20130145.
18. Ogura I, Ono J, Okada Y. Use of cone-beam computed tomography for evaluation of surgical specimen of medication-related osteonecrosis of the jaw. J Oral Maxillofac Radiol 2018; 6: 17-20.
19. Baba A, Goto TK, Ojiri H, Takagiwa M, Hiraga C, Okamura M, et al. CT imaging features of antiresorptive agent-related osteonecrosis of the jaw/medication-related osteonecrosis of the jaw. Dentomaxillofac Radiol 2018; 47: 20170323.
20. Marx RE, Tursun R. Suppurative osteomyelitis, bisphosphonate induced osteonecrosis, osteoradionecrosis: a blinded histopathologic comparison and its implications for the mechanism of each disease. Int J Oral Maxillofac Surg 2012; 41: 283-9.
21. Zirk M, Buller J, Zöller JE, Heneweer C, Kübler N, Lentzen MP. Volumetric analysis of MRONJ lesions by semiautomatic segmentation of CBCT images. Oral Maxillofac Surg 2019; 23: 465-72.